Investigation of Absorption Kinetics by the Phase Plane Method

Aristides Dokoumetzidis[1] and Panos Macheras[2,3]

Received February 17, 1998; accepted May 9, 1998

Purpose. To develop a simple approach for investigating absorption kinetics, which does not require modeling assumptions or intravenous data.

Methods. The concentration (C) -time (t) data are plotted as a phase plane plot (dC/dt *versus* C). Errorless C,t data were generated from one and two compartment models employing first-order, zero-order and Michaelis-Menten input kinetics, and the phase plane plots were constructed. A simple test based on the ratio of slopes of the separate linear regression analyses of absorption and elimination data of the phase plane plot is proposed to justify or not the presence of zero-order input kinetics. Errant data were used to assess the performance of the test developed. Literature data of theophylline and nitroglycerin formulations were analyzed using the phase plane plot. Input rate-time profiles were constructed for one compartment model drugs utilizing the data of the phase plane plot.

Results. The geometric forms of the phase plane plots derived from the errorless data of the various pharmacokinetic models were found to be indicative of the absorption kinetics. Very good results were obtained when the test for the discernment of absorption kinetics was applied to errant data. Zero-order absorption kinetics were justified (i) for the transdermal absorption of nitroglycerin and (ii) only for a certain period of time, for the gastrointestinal absorption of theophylline.

Conclusions. Investigation of absorption kinetics can be accomplished with the phase plane method. The cumulative character of the classical percent absorbed versus time plots can be misleading in justifying the presence of zero-order input kinetics.

KEY WORDS: absorption; absorption kinetics; zero-order; phase plane; phase plane method.

INTRODUCTION

The assessment of *in vivo* drug absorption rates is accomplished with mass balance methods (1–3) and deconvolution techniques (4–6). Mass balance methods require assumptions regarding the model of drug disposition while deconvolution techniques (4–6) assess the input function of the drug but require separate data for the disposition of drug in the body. In addition, deconvolution techniques require computer programs and are based on the assumption that disposition remains constant when the drug is administered orally and intravenously to the same person on different occasions.

Of particular interest in this topic is the assessment of the drug's input rate from controlled-release formulations which have been designed to provide zero-order input into the systemic circulation. A number of methods, such as Wagner-Nelson (1), nonlinear least squares regression (7), function area (8), and modified residual (9) are used to calculate the zero-order absorption rate constant. However, three of these methods (1,7,9) require modeling assumptions while the noncompartmental function area method (8) requires intravenous data.

The aim of the present study is to develop a simple approach for the investigation of absorption kinetics, which does not require modeling assumptions or separate intravenous data. This approach is based on the phase plane plot (dC/dt versus C) using the concentration (C) – time (t) data. Phase plane plots have been used extensively in many areas of research such as non linear dynamics (10), neuroscience (11), brain research (12), physiology (13,14) etc. for the analysis of various kinetic phenomena.

THEORY

In the physical sciences as well as in pharmacokinetics, the traditional strategy to predict the future state of a system is to construct a set of differential equations. In nonlinear dynamics (15–17) the systems are described by means of geometric constructions in which the solution of an "equation of motion" is depicted by a curve in the appropriate space. The coordinate axes necessary for such a plot are the continuum of values of the N-components of the vector $X(t)$ defining the system. This kind of construction is called **phase space** (15–17) and each point in the phase space gives a complete characterization of the dynamical system at a point in time.

Pharmacokinetic models are described by first order ordinary differential equations which involve one variable of the general form $dC/dt = f(C)$ where C is the plasma drug concentration. Therefore, the time evolution of a pharmacokinetic system can be studied by constructing a two dimensional phase plane with coordinates dC/dt and C. This is shown schematically in Fig. 1 utilizing a one-compartment model disposition system with first-order input and elimination, whereas time proceeds from the initial state [dC/dt (4), $C(0)$] to the final state [dC/dt (0), $C(0)$].

Although the phase space graphs are used in nonlinear dynamics to predict the time evolution of the system, pharmacokinetic systems are predictable since they have point attractors (15) i.e. they converge to a single point (zero) in phase space as $t \rightarrow \infty$. However, the shape of the phase plane graphs is indicative of the output and input kinetics. This feature of the phase plane plot is used in the present study for the investigation of input kinetics.

METHODS

Errorless data were generated from the fundamental differential equations defining the various pharmacokinetic models. The one compartment model is described by Eqs. (1), (2) and (3) for first-order, zero-order and Michaelis-Menten input kinetics, respectively. The two compartment model is described by Eqs. (4), (5) and (6) for first-order, zero-order and Michaelis-Menten input kinetics, respectively. In all cases, first-order elimination was assumed. The integrated forms of the differential Eqs. (1–6) were also used for the simulations. Numerical integration was used for the models with Michaelis-Menten kinetics. The corresponding dC/dt versus C plots were constructed.

[1] Department of Physics, University of Athens, Athens, Greece.
[2] Department of Pharmacy, University of Athens, Panepistimiopolis, 15771 Athens, Greece.
[3] To whom correspondence should be addressed. (e-mail: pmahaira@atlas.uoa.gr)

0724-8741/98/0800-1262$15.00/0

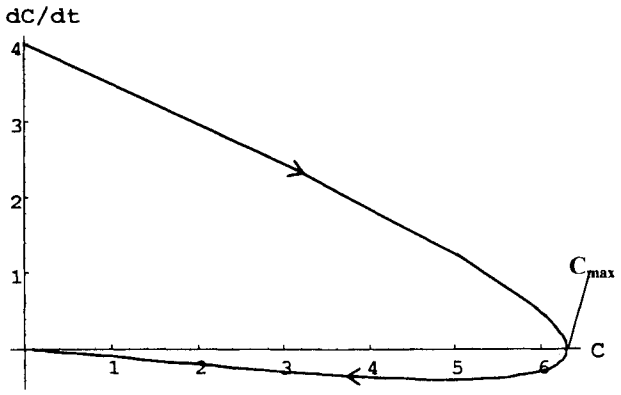

Fig. 1. "Phase plane" plot for a drug obeying one-compartment model disposition with first-order absorption and elimination. The plot was generated from the equations: C = 13.3 ($e^{-0.1t} - e^{-0.4t}$) and dC/dt = 13.3 ($0.4e^{-0.4t} - 0.1e^{-0.1t}$). Time is a continuous parameter which indexes each point along the curve. The time flow is indicated by the arrow, while the x-axis intercept corresponds to C_{max}.

$$\frac{dC}{dt} = \frac{FD}{V} K_a e^{-K_a t} - K_e C \tag{1}$$

$$\frac{dC}{dt} = \frac{FK_0}{V} - K_e C \qquad \text{for } t \leq \tau \tag{2}$$

$$\frac{dC}{dt} = - K_e C \qquad \text{for } t > \tau$$

$$\frac{dC}{dt} = \frac{V_{max} C_g}{K_m + C_g} - K_e C \tag{3}$$

and

$$\frac{dC_g}{dt} = - \frac{V_{max} C_g}{K_m + C_g}$$

$$\frac{dC_1}{dt} = K_a \frac{FD}{V} e^{-K_a t} - K_{10} C_1 - K_{12} C_1 + K_{21} C_2 \tag{4}$$

and

$$\frac{dC_2}{dt} = K_{12} C_1 - K_{21} C_2$$

$$\frac{dC_1}{dt} = \frac{FK_0}{V} - K_{10} C_1 - K_{12} C_1 + K_{21} C_2 \qquad \text{for } t \leq \tau \tag{5}$$

$$\frac{dC_1}{dt} = - K_{10} C_1 - K_{12} C_1 + K_{21} C_2 \qquad \text{for } t > \tau$$

and

$$\frac{dC_2}{dt} = K_{12} C_1 - K_{21} C_2$$

$$\frac{dC_1}{dt} = \frac{V_{max} C_g}{K_m + C_g} - K_{10} C_1 - K_{12} C_1 + K_{21} C_2, \tag{6}$$

$$\frac{dC_2}{dt} = K_{12} C_1 - K_{21} C_2,$$

and

$$\frac{dC_g}{dt} = - \frac{V_{max} C_g}{K_m + C_g}$$

The quantities included in the Eqs. (1–6) are: C is the concentration of the drug in the central compartment; C_1 and C_2 are the concentrations in compartments 1 and 2, respectively; C_g is the concentration of drug in the gastrointestinal tract; K_a is the first-order absorption rate constant; K_0 is the zero-order absorption rate constant; τ is the duration of constant input rate; K_e is the elimination rate constant, K_{10} is the output rate constant from the central compartment; K_{12} and K_{21} are the disposition rate constants; F is the bioavailable fraction; D is the dose; V is the volume of distribution; K_m is the Michaelis-Menten constant, and V_{max} is the maximum velocity.

Noise free data were generated from Eqs. 1, 3, 4 and 6 (first-order and Michaelis-Menten input kinetics) at times t = 0, 0.5, 1, 1.5, 2, 3, 4, 6, 8, 12, 16, 20, and 24 hours; noise free data were also generated from Eqs. 2 and 5 (zero-order input kinetics) at times t = 0, 2, 4, 6, 8, 10, 12, 16, 20, 24, 28, and 32 hours, while constant rate of input was assumed for the first 12 h. The following values were assigned to the parameters: K_0 = 10 mg h^{-1}, V = 100 L, F = 1, K_m = 120 mg/L, V_{max} = 100 mg/L/h, K_a = 0.4 h^{-1}, and K_e = 0.1 h^{-1} or K_e = 0.3 h^{-1}. For each one of the models, one thousand sets with superimposed normally distributed error with coefficient of variation (CV) of 5% or 10% were prepared from the noise free sets.

The contaminated simulated data were analyzed by calculating the derivative dC/dt numerically while the corresponding midpoint concentration, C, value was used for plotting purposes i.e. *dC/dt versus C*.

The same procedure was applied to real experimental data taken from literature.

RESULTS AND DISCUSSION

Errorless Data. The errorless data were used to provide a pictorial view of the plot *dC/dt versus C* for one compartment model (Fig. 2) and two compartment model drugs (Fig. 3). Fig. 2 and 3 provide the phase plane of the systems under study i.e. the space of all possible states of the systems (18). These figures visualize the dynamics of the systems since the ($dC/dt, C$) plane provides the "position" (concentration) and "speed" (rate) of the drug in plasma at every point. For our purposes, however, the shapes of the curves in Figs. 2 and 3 and their topological properties are important. For example, the curves in Fig. 2A and 2C are equivalent from a topological viewpoint since they can be smoothly deformed to each other. On the contrary, the lines of Fig. 2B are not equivalent with either the curves of Fig. 2A or Fig. 2C. This topological dissimilarity arises from the qualitative change (18) of the input rate in the zero-order system (see Eq. 2). The discontinuity involved in the zero-order system comprises and is reflected to the fundamental difference between the continuous curves of Figs. 2A and 2C and the discontinuous lines of Fig. 2B. These observations are also applicable to the two compartment model systems (compare Fig. 3B with Figs. 3A and 3C).

When first-order or Michaelis-Menten absorption kinetics are encountered, the phase plane plots concave downwards during the absorption phase and upwards during the elimination phase, Figs. 2A, 2C, 3A, and 3C. The y-intercepts and the initial and terminal slopes of the curves are given in the Appendix. It

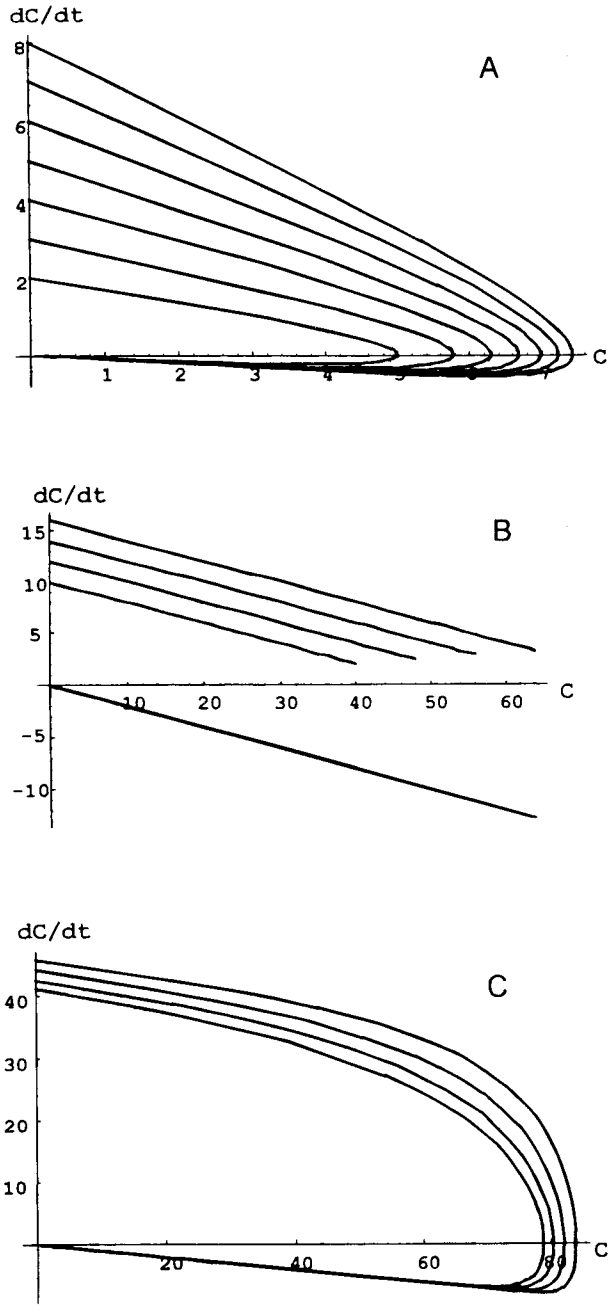

Fig. 2. "Phase plane" plot for a drug obeying one-compartment model disposition with first-order (A), zero-order (B) and Michaelis-Menten (C) absorption and first order elimination. The plots were generated from: Eq. 1 using FD/V = 10 and K_e = 0.1; the values for K_a from top to bottom are: 0.8, 0.7, 0.6, 0.5, 0.4, 0.3 and 0.2. (A) Eq. 2 using F/V = 10 and K_e = 0.2; the values for K_0 from top to bottom are: 1.6, 1.4, 1.2 and 1. (B) Eq. 3 using numerical integration with V_{max} = 50, K_e = 0.1 and $C_g(t = 0)$ = 100; the values for K_m from top to bottom are 10, 14, 18 and 22 (C).

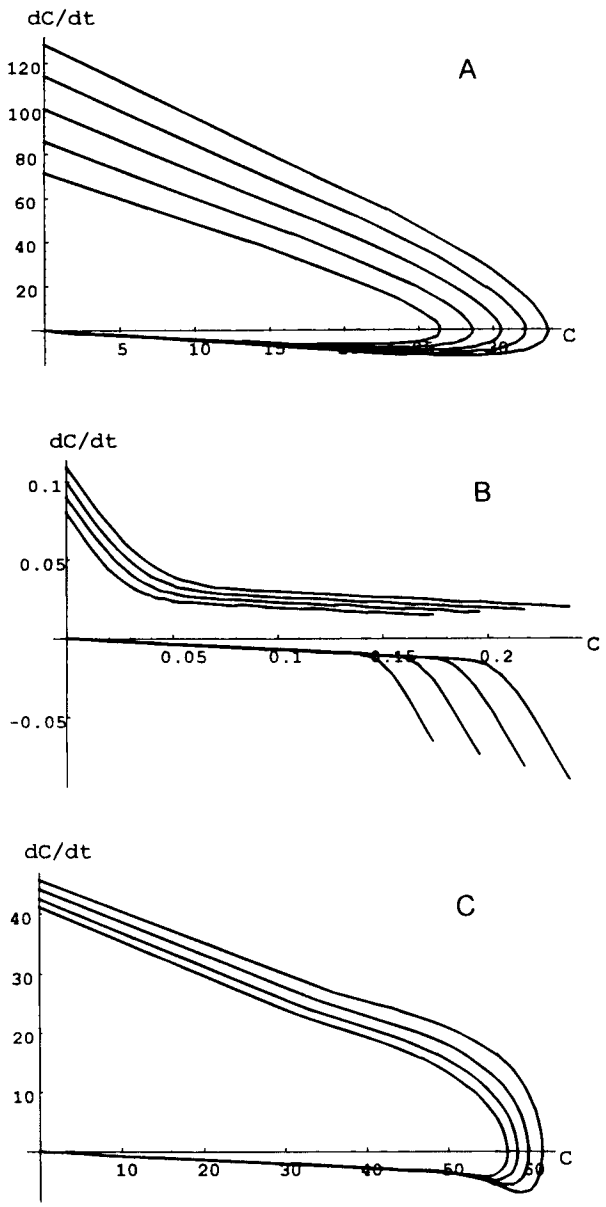

Fig. 3. "Phase plane" plot for a drug obeying two-compartment model disposition with first-order (A), zero-order (B) and Michaelis-Menten (C) absorption and first order elimination. The plots were generated from: Eq. 4 using F = 1, D = 500, V = 7, K_{12} = 0.6, K_{21} = 1.2, K_{10} = 0.66; the values for K_a from top to bottom are 1.8, 1.6, 1.4, 1.2 and 1. (A) Eq. 5 using (F/V = 0.02, K_{12} = 1.86, K_{21} = 1, K_{10} = 0.21 and τ = 8; the values for K_0 from top to bottom are 5.5, 5, 4.5 and 4. (B) Eq. 6 using numerical integration with V_{max} = 50, K_{10} = 0.1, K_{12} = 0.6, K_{21} = 1.2 and $C_g(t = 0)$ = 100; the values for K_m from top to bottom are 10, 14, 18 and 22 (C).

is interesting to note that the ratio of the initial slope to the terminal slope of the curve of the one-compartment model with first-order kinetics is greater than or at least equal to 2 (see Appendix). Also, in the one compartment model with Michaelis-Menten input kinetics, Fig. 2C, the ratio of the initial to the terminal slope i.e.

$$\left[\frac{V_{max}K_m}{(K_m + C_g(t = 0))^2} + K_e\right] \Big/ K_e$$

(see Appendix) is larger than one. Since there is no explicit expression in terms of time for the slope of the curve during the absorption phase, we calculated the slope numerically and found that the ratio of the slopes is progressively becoming much larger as time approaches t_{max}. This finding is in accord with the visual inspection of the plots in Fig. 2C.

Figure 2B shows the phase plane plot of a one compartment model system with zero-order absorption kinetics. It consists of two straight lines which are in accord with Eq. 2. The two slopes are equal and correspond to the elimination rate constant (see Appendix).

Figure 3B shows the phase plane plot of a two compartment model system with zero-order absorption kinetics. Although the plot is not linear, two symmetrical limbs are observed while discontinuity is again the prevailing feature of the zero-order input kinetics. The y-intercept and the initial and terminal slopes of the curves in Fig. 3B are given in the Appendix.

Errant Data. In the one-compartment model with zero-order absorption, the phase plane plot (Fig. 2B) has two unique characteristics, namely i) discontinuity between the absorption and the elimination phase and ii) the two limbs of the graph are linear with equal slopes. These characteristics, coupled with the nonlinear character of all other plots, prompted us to design the following simple test for the discernment of absorption kinetics for a given data set. The data are initially segmented in two parts i.e. absorption and elimination phase data. Linear regression analysis is performed separately for absorption and elimination phase data using the pairs (dC/dt, C) where C is the mid-point concentration. The ratio of the two slopes is calculated and compared with 2. This value is the theoretical minimum for the ratio of the slopes of the initial and terminal limbs of the curve for the one-compartment model with first-order absorption, (Fig. 1A and Appendix). For the reasons delineated in the "errorless data" section, a high ratio of slopes can be also anticipated with data obeying one-compartment model with Michaelis-Menten input kinetics. This conclusion is further substantiated by the fact that the visual inspection of the shape of the curves in Fig. 1A and 1C reveals that the ratio of slopes will be attenuated since the absorption phase data concave downwards while the elimination phase data concave upwards. Consequently, when the ratio of slopes is higher than 2 the possibility of zero-order absorption kinetics is ruled out while values lower than 2 are indicative of zero-order input kinetics.

To confirm these observations the errant data were analyzed as described. Table I shows, for each model, the number of successes (out of 1000 trials) to comply with the criterion of the ratio of slopes. It is clear that for both one and two compartment models, zero-order kinetics is not justified when first-order or Michaelis-Menten kinetics is operating with random error either 5% or 10% *CV*. Three different sets of 1000 trials were analyzed for one compartment model with zero-order absorption. Set I corresponds to the sampling schedule described and everything goes as expected. For set II though, the datum point with t = 12 h was not taken into account. This caused serious aggravation of the results since at time t = 12 h the constant input is terminated. Set III is again without the datum point at t = 12 h but the midpoint generated from the two surrounding data points is excluded from the calculations. This approach fixes things up and is indicative of how this tool must be used with a real data set. This means that caution should be exercised with data points close to C_{max} in order to avoid misclassifications of the data in the two phases. Besides, the approach developed exhibited good (2.5%) and moderate (17.9%) performance for the justification of zero-order kinetics in the two compartment model at lower (CV = 5%) and higher (CV = 10%) random error level, respectively, despite of the nonlinear character of the plot, Fig. 3B. It is most likely that this result is associated with the symmetry of this plot above and below the x-axis.

Table I. Number of Successes (Ratio of Slopes >2) with 1000 Different Random Sets of Data for Each Model

Model	Input kinetics	Set	K_a/K_e	CV = 5%	CV = 10%
One compartment	First-order		0.4/0.1	1000	992
			0.4/0.3	1000	995
	Zero-order	I		0	6
		II		101	216
		III		0	2
	Michaelis-Menten			1000	986
Two compartment	First-order			1000	1000
	Zero-order			25	179
	Michaelis-Menten			1000	996

Apart from the aforementioned analysis, one should also mention that the visual inspection of the phase plane plot of the experimental data can be helpful for the justification of zero-order kinetics. Some examples of errant data are shown in Fig. 4. The lines connecting the data points in Figs. 4 and 5 have been drawn to facilitate the reader to follow the time flow which is clockwise from positive to negative values of dC/dt. Visual inspection of Fig. 4 reveals that only the data, which obey zero-order input kinetics (Fig. 4C and 4D), exhibit (i) patent discontinuity (even though lines connecting data points are present) between the two phases and (ii) similar slopes for the data above and below the x-axis.

Literature Data. In this section real experimental data of theophylline (19) and nitroglycerin (20) are used to demonstrate the application of the phase plane method in the analysis of absorption kinetics.

The first study (19) examines the effect of a high-fat breakfast on theophylline absorption from the sustained release formulation Theo-Dur Sprinkle. In this study (19), 6 subjects received 900 mg of Theo-Dur Sprinkle under fasting conditions and immediately after a high-fat breakfast. Figures 5A and 5B show the phase plane plots obtained from the two sets of theophylline experimental data. These plots reveal that the values of dC/dt initially increase and then decrease with concentration during the absorption phase indicating that the assumptions of either zero- or first-order rate of absorption are invalid. This kind of behavior has been noted in a great number of deconvolution studies and is associated with the stochastic nature of drug's absorption from the gastrointestinal tract (21). However, if one ignores the first datum point of the absorption phase in Fig. 5A and 5B and applies linear regression to the next four data points, i.e. data from 1 to 4.5 hours, one obtains

for Figure 5A: $dC/dt = 2.46 - 0.057\ C$
for Figure 5B: $dC/dt = 0.91 - 0.041\ C$

The corresponding slopes of the elimination phase data in Fig. 5A and 5B are, −0.055 and −0.041, respectively. The similarity

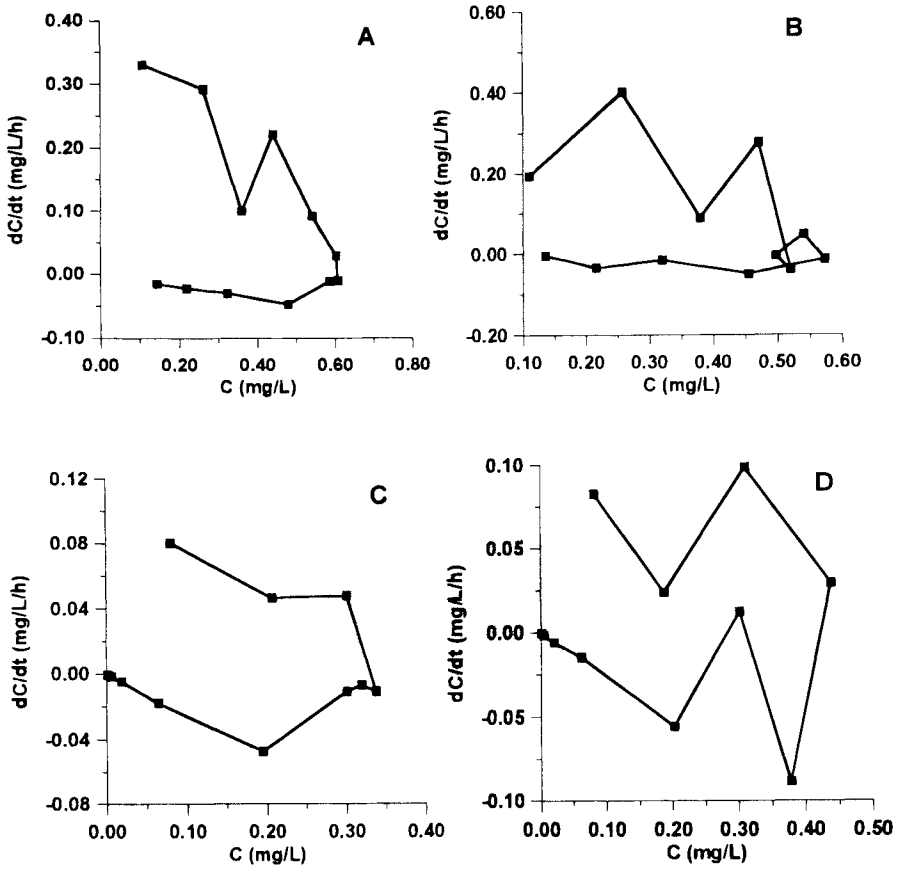

Fig. 4. Some examples of the phase plane plots of the errant data generated. The plots correspond to a drug with one compartment model disposition with first-order absorption (A and B) or zero-order absorption (C and D). Plots A and C have superimposed error of CV = 5% while in plots B and D, CV = 10%.

of the slopes in both cases demonstrate that zero-order kinetics is operating only for the first 4.5 hours, apart from a short initial increase of input rate.

The nitroglycerin data were obtained from an *in vivo* study of a transdermal system (Nitro-Dur) which was designed to deliver the drug with constant rate of input for 12 h (20). The phase plane plot of nitroglycerin data, exhibits clearly the abrupt discontinuation of the absorption process and the almost parallel change of *dC/dt* as a function of concentration in both phases, Fig. 5C. In fact, the ratio of slopes of the two best straight lines utilizing separately all data points from both phases is 1.65. This value substantiates further the view of zero-order input kinetics for nitroglycerin despite the fluctuations of rate in the absorption phase and the limited number of data points of the elimination phase.

The Phase Plane, the Input Rate and the Wagner-Nelson (1) Method. In this section the phase plane plot is considered in conjunction with the relevant approaches used for the construction of the input rate and the Wagner-Nelson (1) plot. The main purpose of this section is to demonstrate that the apparent linearity of Wagner-Nelson plots can mask the detailed features of the rate of input. To this end, drugs with one-compartment model disposition are considered. For these drugs Eqs. 1–3 can be written in a generalized form expressing input rate in concentration/time units:

$$\frac{dC}{dt} = \text{input rate} - K_e\, C \tag{7}$$

or

$$\text{input rate} = \frac{dC}{dt} + K_e\, C \tag{8}$$

Obviously, Eq. 8 holds for any type of input kinetics provided that one-compartment model disposition is assumed. According to Eq. 8 the input rate at each time t can be estimated by adding the corresponding elimination rate (K_eC) to the algebraically calculated change of plasma drug concentration *dC/dt*. The required estimate for K_e can be obtained from the conventional semilogarithmic plot of the terminal concentration-time data points of the elimination phase in the same way that it is applied routinely (1). Finally, the input rate-time profile can be obtained by plotting the input rate *versus* the midpoints t of the blood sampling intervals.

The methodology is analogous to the Loo-Riegelman technique (3) i.e. utilizing rates of change in systemic concentrations over finite intervals. However, the technique allows one to construct a fictitious "cumulative concentration-time" profile, by calculating (using the trapezoidal rule) the area under the curve of the input rate for each time interval. This fictitious quantity represents the plasma concentration of the absorbed drug if elimination is ignored. When each of these quantities

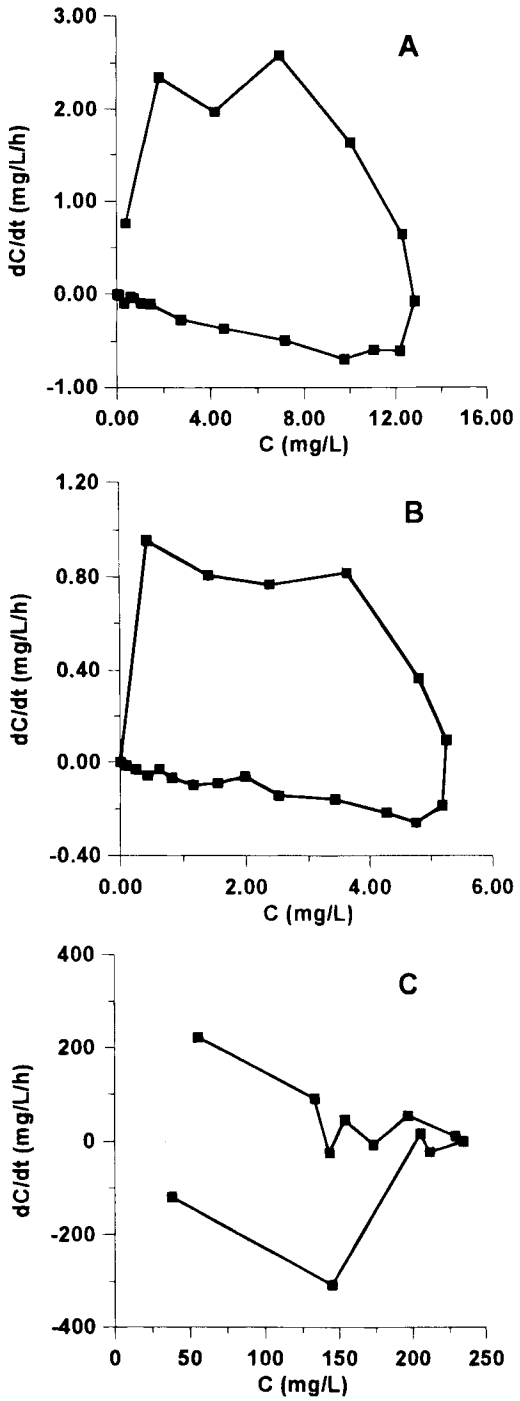

Fig. 5. Phase plane plots for the data obtained from the literature. Plots A and B correspond to theophylline (19) under fasting conditions (A) and immediately after a high-fat breakfast (B). Plot C corresponds to a transdermal nitroglycerin data set (20).

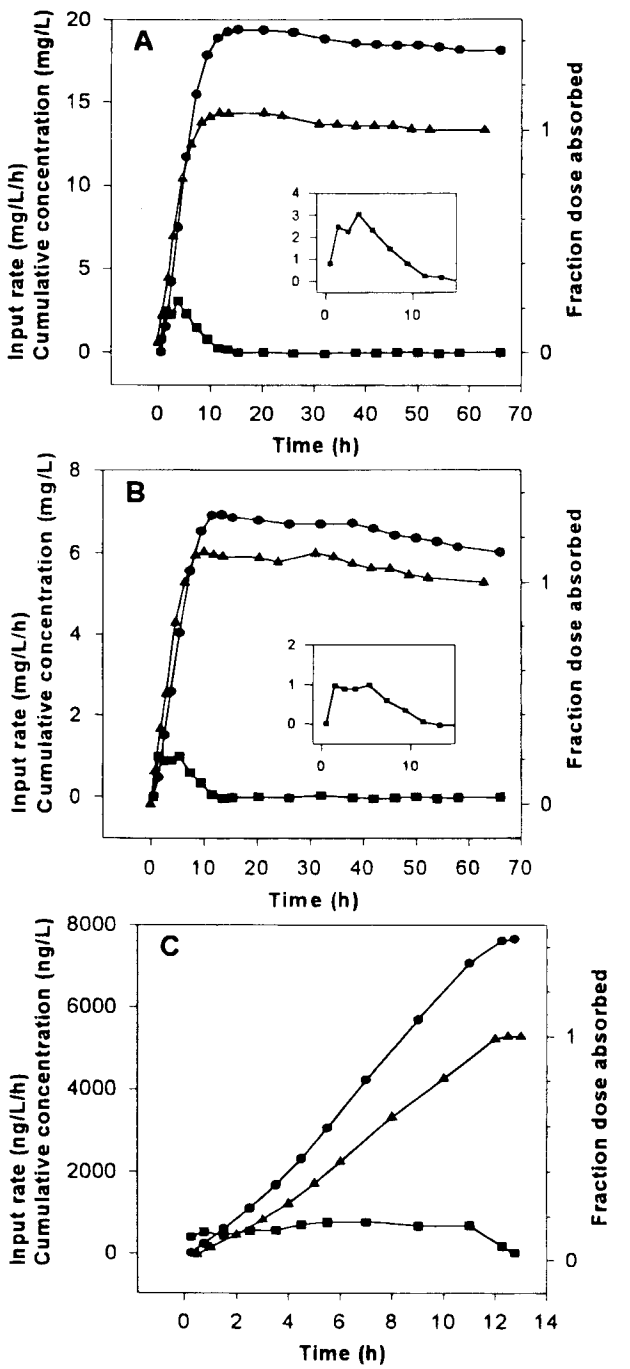

Fig. 6. Input rate-time plots (squares, left-hand ordinate), "cumulative concentration"-time plots (circles, left-hand ordinate) and Wagner-Nelson plots (triangles, right-hand ordinate) of the corresponding data sets A, B and C of Figure 5. The slight decline of the plateau of theophylline cumulative concentration—time plots is associated with the underestimation of the elimination rate constant K_e used in Eq. 8. The insets magnify the absorption phase of the input rate—time profile of theophylline.

is divided by the total area, the normalized fictitious cumulative concentration-time profile obtained has all the qualitative features of the classical percent absorbed versus time plots. Figure 6 shows the cumulative concentration-time profiles for theophylline (19) and nitroglycerin (20) data along with the corresponding input rate-time profiles. The apparent linearity of the cumulative plots in Fig. 6 during the absorption phase is usually explained as a clear indication of zero-order input kinetics. However, the co-plotted input rates support such a conclusion only for nitroglycerin and not for the entire period of theophylline absorption (see insets of Fig. 6). It seems likely that the fictitious concentration-time profiles as well as the equivalent

Wagner-Nelson (1) plots (Fig. 6), which are both of cumulative nature, cannot unmask the detailed features of the input rate. In fact, the correlation coefficients of the ascending limbs of the Wagner-Nelson plots and the cumulative concentration-time profiles are 0.996, 0.989, 0.997, and 0.993 for the data of Fig. 6A and 6B, respectively. As it was mentioned above, these results are usually explained as indications of zero-order input kinetics. On the contrary, the contrast of the cumulative concentration-time profile with the input rate-time profile allows one to validate his (her) conclusions for the type of the input kinetics for one-compartment model drugs.

On the whole, however, it is advisable to use the phase plane plot as a single tool for the investigation of absorption kinetics since (i) the input rate-time profile is derived from the corresponding phase plane plot assuming one-compartment model disposition and (ii) no modeling assumptions are required for the construction of the phase plane plots.

CONCLUSIONS

The method based on the phase plane plot is a convenient and reliable method to investigate the characteristics of input kinetics. It does not rely on modeling assumptions while minimum computation is required. Finally, the method can be used as an adjunct to the various methods used for the assessment of input kinetics employing various assumptions (1–9).

ACKNOWLEDGMENTS

Supported in part by the General Secretariat for Research and Technology (PENED Grant 70/3/2824).

APPENDIX

One Compartment Model with First-Order Absorption and Elimination. (Eq. 1)

Let

$$\dot{C} = \frac{dC}{dt} \text{ and } \ddot{C} = \frac{d^2C}{dt^2}$$

then the slope of the dC/dt vs C curve is

$$\frac{d\dot{C}}{dC} = \frac{d\dot{C}}{dt}\frac{dt}{dC} = \frac{d\dot{C}}{dt} \Big/ \frac{dC}{dt} = \frac{\ddot{C}}{\dot{C}} \qquad (1A)$$

Where

$$\dot{C} = \frac{FD}{V}\left[K_a e^{-K_a t} - \frac{K_e K_a}{K_a - K_e}(e^{-K_e t} - e^{-K_a t})\right] \qquad (2A)$$

Derivation of Eq. 2A provides $\ddot{C}$. After the calculations we end up with

$$\text{slope}(t) = \frac{\ddot{C}}{\dot{C}} = \frac{-e^{(K_a + K_e)t} K_a^2 + e^{2K_a t} K_e^2}{e^{(K_a + K_e)t} K_a - e^{2K_a t} K_e}$$

which gives the slope at any time t. For t = 0 the initial slope is:

$$\text{slope}(0) = -(K_a + K_e).$$

For the special case, $K_a = K_e = K$, the equation of the model is

$$C = \frac{FD}{V} Kte^{-Kt}$$

Therefore,

$$\text{slope}(t) = \frac{\ddot{C}}{\dot{C}} = \frac{-2K + K^2 t}{1 - Kt}$$

and

$$\text{slope}(0) = -2K$$

For the terminal slope, the calculation of the limit as t goes to infinity is required. Three separate cases are considered:
a) $K_a > K_e$

$$\text{slope}(\infty) = \lim_{t\to\infty} \frac{\ddot{C}}{\dot{C}} = \lim_{t\to\infty} \frac{-e^{(K_a + K_e - 2K_a)t} K_a^2 + K_e^2}{e^{(K_a + K_e - 2K_a)t} K_a - K_e} = -K_e$$

b) $K_a < K_e$

$$\text{slope}(\infty) = \lim_{t\to\infty} \frac{\ddot{C}}{\dot{C}} = \lim_{t\to\infty} \frac{-K_a^2 + e^{(2K_a - K_e - K_a)t} K_e^2}{K_a - e^{(2K_a - K_e - K_a)t} K_e} = -K_a$$

c) $K_a = K_e = K$

$$\text{slope}(\infty) = \lim_{t\to\infty} \frac{\ddot{C}}{\dot{C}} = -K$$

The intercept of the "phase line" with the dC/dt axis, is the value of dC/dt at t = 0. Using Eq. 2A with t = 0:

$$\dot{C}(t = 0) = \frac{FD}{V} K_a \text{ when } K_a \neq K_e$$

$$\dot{C}(t = 0) = \frac{FD}{V} K \text{ when } K_a = K_e = K$$

In an analogous manner the following slopes and intercepts were calculated for the various models.

One Compartment Model with Zero-Order Absorption and First-Order Elimination. (Eq. 2)

$$\text{Slope of the absorption phase} = -K_e$$

$$\text{Slope of the elimination phase} = -K_e$$

$$\text{Intercept: } \dot{C}(t = 0) = \frac{F}{V} K_0$$

One Compartment Model with Michaelis-Menten Absorption and First-Order Elimination. (Eq. 3)

$$\text{Slope}(0) = -\frac{V_{max} K_m}{(K_m + C_g(t = 0))^2} - K_e$$

$$\text{Slope}(\infty) = -K_e$$

$$\text{Intercept: } \dot{C}(t = 0) = \frac{V_{max} C_g(t = 0)}{K_m + C_g(t = 0)}$$

Two Compartment Model with First-Order Absorption and Elimination. (Eq. 4)

$$\text{Slope}(0) = -(K_a + K_{10} + K_{12})$$

$$\text{Slope}(\infty) = -\lambda_2$$

Where λ_2 is the smaller ($\lambda_2 < \lambda_1$) hybrid rate constant.

$$\text{Intercept: } \dot{C}(t = 0) = \frac{FD}{V} K_a$$

Two Compartment Model with Zero-Order Absorption and First-Order Elimination. (Eq. 5)

$$\text{Slope}(0) = -(K_{10} + K_{12})$$

$$\text{Slope}(\infty) = -\lambda_2$$

$$\text{Intercept: } \dot{C}(t = 0) = \frac{F}{V} K_0$$

Two Compartment Model with Michaelis-Menten Absorption and First-Order Elimination. (Eq. 6)

$$\text{Slope}(0) = -\frac{V_{max} K_m}{(K_m + C_g(t = 0))^2} - K_{10} - K_{12}$$

$$\text{Slope}(\infty) = -\lambda_2$$

$$\text{Intercept: } \dot{C}(t = 0) = \frac{V_{max} C_g(t = 0)}{K_m + C_g(t = 0)}$$

REFERENCES

1. J. G. Wagner and E. Nelson. Per cent absorption time plots derived from blood level and urinary excretion data. *J. Pharm. Sci.* **52**:610–611 (1963).
2. J. G. Wagner. Application of the Wagner-Nelson absorption method to the two compartment open model. *J. Pharmacokin. Biopharm.* **2**:469–486 (1974).
3. J. C. K. Loo and S. Riegelman. New method for calculating the intrinsic absorption rate of drugs. *J. Pharm. Sci.* **57**:918–928 (1968).
4. P. Veng-Pedersen. Internal deconvolution — a method for evaluating *in vivo* release, *in vivo—in vitro* correlation, and drug absorption, not requiring separate reference administration. *Pharm Res.* **12**:S-369 (1995).
5. F. Podczeck, K. M. Charter, M. Newton, and K. Yuen. Calculation of the drug absorption rates of two sustained-release theophylline formulations using quantified maximum entropy. *Eur. J. Pharm. Biopharm.* **41**:254–261 (1995).
6. Z. Yu, S. S. Hwang, and K. S. Gupta. DeMonS-A new deconvolution method for estimating drug absorbed at different time intervals and/or drug disposition model parameters using a monotonic cubic spline. *Biopharm. Drug Dispos.* **18**:475–487 (1997).
7. C. M. Metzler, G. K. Elfring, and A. J. McExen. A package of computer programs for pharmacokinetic modeling. *Biometr.* **30**:562 (1974).
8. H. Cheng and W. J. Jusko. The area function method for assessing the drug absorption rate in linear systems with zero-order input. *Pharm Res.* **6**:133–139 (1989).
9. X. Liu, K R. Brouwer, and G. M. Pollack. A modified residual method to estimate the zero order absorption rate constant in a one compartment model. *Biopharm. Drug Dispos.* **18**:93–101 (1997).
10. D. B. Marghitu, S. A. Kincaid, and P. F. Rumph. Nonlinear dynamics stability measurements of locomotion in health greyhounds. *Am. J. Vet. Res.* **57**:1529–1535 (1996).
11. O. Tchernichovski and I. Golani. A phase plane representation of rat exploratory behavior. *J. Neurosci. Methods.* **62**:21–27 (1995).
12. J. D. Cooke and S. H. Brown. Phase plane tracking: a new method for shaping movements. *Brain Res. Bull.* **16**:435–437 (1986).
13. H. S. Karagueuzian, S. S. Khan, T. A. Denton, M. Gotoh, W. J. Mandel, and G. A. Diamond. Phase plane plot of electrograms as a marker of ventricular electrical instability during acute ischemia: initial experimental results and potential clinical applications. *Pacing Clin. Electrophysiol.* **15**:2188–2193 (1992).
14. A. Fonseca-Costa, P. Magrassi, W. A. Zin, and L. J. M. Romeo Jr. Detection and quantification of small right-to-left shunts by the phase-plane method. *Am. J. Physiol.* **247**:H517–H522 (1984).
15. J. M. van Rossum, J. E. G. M. de Bie, G. van Lingen, and H. W. A. Teeuwen. Pharmacokinetics from a dynamical systems point of view. *J. Pharm. Biopharm.* **17**:365 (1989).
16. P. Macheras, P Argyrakis, and C. Polymilis. Fractal geometry, fractal kinetics and chaos en route to biopharmaceutical sciences. *Europ. J. Drug Metab. Pharmacok.* **21**:77–86 (1996).
17. S. Wiggins. Introduction to applied nonlinear dynamical systems and chaos. Springer-Verlag, New York, 1990.
18. A Garfinkel. Mathematics for physiology. *Am. J. Physiol.* **245**:R455–R466, (1983).
19. A. Yakobi and E. Halperin Valega. Oral sustained release formulations: Design and Evaluation. Pergamon Press, New York, p.166, 1988.
20. E. A. Cefali, C. R. Banfield, M. A. Gonzalez, and J. G. Wagner. In vivo determination of zero-order absorption from transdermal glycerol trinitrate system. *Eur. J. Pharm. Biopharm.* **39**:140–143 (1993).
21. P. Veng-Pedersen and N. B. Modi. Optimal extravascular dosing intervals. *J. Pharmacokin. Biopharm.* **19**:405–412 (1991)